A-MuLV–transformed pre–B cells resulted from the activation of Jak1 and Jak3 in the absence of cytokines. Jak1 and Jak3 were activated in Clone K cells treated with IL-7, whereas in A-MuLV–transformed pre–B cell lines, these kinases were constitutively active (Fig. 3) (*11*). In pre–B cells transformed with a temperature-sensitive mutant of v-*abl*, Jak1 and Jak3 were active at permissive temperatures, and upon a shift to nonpermissive temperatures, they became inactive (Fig. 3). Thus, in A-MuLV–transformed pre–B cells, the activities of Jak1 and Jak3 correlate with that of the v-Abl protein tyrosine kinase.

We next investigated the possible interaction between v-Abl and Jak1 or Jak3. Jak1 or Jak3 was immunoprecipitated from extracts of pre–B cells expressing the temperature-sensitive mutant of v-Abl. The v-Abl protein was detected in Jak1 and Jak3 immune complexes (Fig. 4) (*21*). Jak1 was also detected in v-Abl immunoprecipitates (Fig. 4B). These observations were confirmed with several other antibodies to Jak1 and Jak3 (*11*). We were unable to coimmunoprecipitate either Jak1 or Jak3 with the 150-kD c-Abl protein in the non–A-MuLV–transformed pre–B cell line Clone K (Fig. 4).

Two models have been proposed for the mechanism of growth factor independence in cells transformed by oncogenic forms of Abl (*5, 7, 22, 23*). According to one model, v-*abl* may increase the synthesis of RNAs encoding cytokines. Secreted cytokines could then bind their receptors and transduce their signals. Alternatively, v-Abl may abrogate the need for cytokines to bind to their receptors by interacting with components of cytokine signal transduction pathways. In an attempt to distinguish between the two models, we assessed the amount of RNA encoding IL-4 and IL-7 in the pre–B cells transformed with the temperature-sensitive mutant of v-*abl*. We were unable to detect IL-4 or IL-7 mRNAs by reverse transcription–polymerase chain reaction (RT-PCR) in these cells (*11*). In addition, supernatants from cultures of A-MuLV–transformed pre–B cell lines did not induce GAS binding activities in Clone K cells (*11*). Although, we cannot exclude the possibility that these transformed cells produce other cytokines, the lack of mRNA for IL-4 and IL-7 and our observation that Jak1 and Jak3 coimmunoprecipitate with v-Abl are consistent with the latter model. Our results suggest that A-MuLV constitutively activates the IL-4 and IL-7 signaling pathways. Constitutive activation of Jak-STAT signaling has also been observed in T cells transformed with human T cell leukemia virus–I (*24*). Activation of cytokine signal transduction pathways might be a mechanism by which some transforming viruses induce proliferation of their target cells.

REFERENCES AND NOTES

1. J. B. Konopka and O. N. Witte, *Biochim. Biophys. Acta* **823**, 1 (1985); N. Rosenberg, *Semin. Cancer Biol.* **5**, 95 (1994).
2. A. Shields *et al.*, *Cell* **18**, 955 (1979).
3. R. J. Prywes *et al.*, *J. Virol.* **54**, 114 (1985); E. T. Kipreos and J. Y. Wang, *Oncogene Res.* **2**, 277 (1988); B. J. Mayer *et al.*, *Mol. Cell. Biol.* **12**, 609 (1992); Y. Y. Chen and N. Rosenberg, *Proc. Natl. Acad. Sci. U.S.A.* **89**, 6683 (1992); B. J. Mayer and D. Baltimore, *Mol. Cell. Biol.* **14**, 2883 (1994).
4. A. Engelman and N. Rosenberg, *J. Virol.* **64**, 4242 (1990); *Mol. Cell. Biol.* **10**, 4365 (1990).
5. J. H. Pierce *et al.*, *Cell* **41**, 685 (1985); W. D. Cook, B. Fazekas De St. Groth, J. F. A. P. Miller, H. R. McDonald, R. Gabathuler, *Mol. Cell. Biol.* **7**, 2631 (1987).
6. P. W. Kincade, G. Lee, C. E. Pietrangeli, S. Hayashi, J. M. Gimble, *Annu. Rev. Immunol.* **7**, 111 (1989).
7. J. C. Young, M. L. Gishizky, O. N. Witte, *Mol. Cell. Biol.* **11**, 854 (1991).
8. J. E. Darnell Jr., I. M. Kerr, G. R. Stark, *Science* **264**, 1415 (1994); J. N. Ihle *et al.*, *Trends Biochem. Sci.* **19**, 222 (1994).
9. S. Pellegrini and C. Schindler, *Trends Biochem. Sci.* **18**, 338 (1993).
10. C. A. Whitlock *et al.*, *Cell* **32**, 903 (1983); P. Hunt *et al.*, *ibid.* **48**, 997 (1987); C. A. Whitlock *et al.*, *ibid.*, p. 1009.
11. N. N. Danial, unpublished data.
12. Y. Y. Chen *et al.*, *Genes Dev.* **8**, 688 (1994).
13. The trypan blue uptake test for viability showed that the viability of pre–B cells transformed with the temperature-sensitive mutant of v-*abl* after being shifted to nonpermissive temperatures did not decrease. These cells also express the human BCL-2 protein and can survive more than 2 weeks at nonpermissive temperatures (*12*).
14. A. Pernis *et al.*, *J. Biol. Chem.* **270**, 14517 (1995).
15. J.-X. Lin *et al.*, *Immunity* **2**, 331 (1995).
16. C. Schindler *et al.*, *EMBO J.* **13**, 1350 (1994).
17. P. Rothman *et al.*, *Immunity* **1**, 457 (1994).
18. J. Hou *et al.*, *ibid.* **2**, 321 (1995); F. W. Quelle *et al.*, *Mol. Cell. Biol.* **15**, 336 (1995).
19. J. Hou *et al.*, *Science* **265**, 1701 (1994).
20. M. Müller *et al.*, *Nature* **366**, 129 (1993); O. Silvennoinen *et al.*, *ibid.*, p. 583.
21. Extracts from 18.81A20 cells were immunoprecipitated with antibodies against either Jak1 (directed to amino acids 797 to 817), Jak3 [directed to amino acids 1104 to 1124], or Abl (directed to the COOH-terminus of the Abl protein), and the immunoprecipitates were immunoblotted with a monoclonal antibody to Abl (Oncogene Science). Analysis by densitometry suggested that Jak3 and Jak1 immunoprecipitates contained ~10 to 20% of the v-Abl proteins found in the Abl immunoprecipitations. We find that the v-Abl antibody depletes ~90% of total cellular v-Abl from the 18.81A20 extracts. Coimmunoprecipitation of these proteins was not disturbed by increasing the NaCl concentration to 1M or by adding 0.1% SDS.
22. W. D. Cook *et al.*, *Cell* **41**, 677 (1985).
23. I. K. Hariharan, S. Cory, J. M. Adams, *Oncogene Res.* **3**, 387 (1988).
24. T.-S. Migone *et al.*, *Science* **269**, 79 (1995).
25. F. W. Alt *et al.*, *Cell* **27**, 381 (1981).
26. O. R. Colamonici *et al.*, *J. Biol. Chem.* **269**, 3518 (1994).

27. We thank C. W. Schindler and S. P. Goff for critical reading of this manuscript and helpful discussions, N. Rosenberg for the pre–B cell line transformed with the temperature-sensitive mutant of v-*abl*, J. Ihle for Jak1 antibody, J. O'Shea for Jak3 antibody, S. P. Goff for Abl antibody, and S. Gupta for technical suggestions. Supported by NIH grants AI 33540-02 (P.B.R.), the Pew Scholars Program (P.B.R.), and Pfizer Incorporated (P.B.R.).

7 March 1995; accepted 6 July 1995

Lateral Interactions in Primary Visual Cortex: A Model Bridging Physiology and Psychophysics

Martin Stemmler,* Marius Usher,† Ernst Niebur‡

Recent physiological studies show that the spatial context of visual stimuli enhances the response of cells in primary visual cortex to weak stimuli and suppresses the response to strong stimuli. A model of orientation-tuned neurons was constructed to explore the role of lateral cortical connections in this dual effect. The differential effect of excitatory and inhibitory current and noise conveyed by the lateral connections explains the physiological results as well as the psychophysics of pop-out and contour completion. Exploiting the model's property of stochastic resonance, the visual context changes the model's intrinsic input variability to enhance the detection of weak signals.

A characteristic feature of primary visual cortex (V1) in primates is its topographic organization into columns (*1*) of neurons responding to oriented stimuli within restricted regions of the visual field. A neuron's classical receptive field (CRF) is defined as that region of visual space in which an individual stimulus will elicit a response. Neuroanatomical studies (*2*), however, have revealed an extensive network of long-range horizontal processes that extend far beyond the representation of the classical receptive field in cortex. While these lateral connections primarily link regions of cortex whose neurons prefer stimuli with similar orientations, the contribution of these connections in the processing of visual information remains unclear. Gilbert

M. Stemmler and E. Niebur, Computation and Neural Systems Program, 139-74, California Institute of Technology, Pasadena, CA 91125, USA.
M. Usher, Department of Psychiatry, University of Pittsburgh, Pittsburgh, PA 15260, and Department of Psychology, Carnegie-Mellon University, Pittsburgh, PA 15213, USA.

*To whom correspondence should be addressed.
†Present address: Department of Psychology, University of Kent at Canterbury, Cambridge, CT2 7NZ, UK.
‡Address after 1 November 1995: Krieger Mind/Brain Institute and Department of Neuroscience, Johns Hopkins University, 3400 North Charles Street, Baltimore, MD 21218, USA.

(3), for instance, has suggested that the plexus of horizontal connections provides neurons with information about the visual context of a stimulus.

The meaning of visual context can be illustrated with two examples drawn from common experience. Suppose the visual scene consists of a large wheat field. Individual stalks of wheat pale in importance compared to the wheat field as a whole. Only a feature in the scene that is "different" should stand out—for example, a horizontal bench among vertical stalks—which corresponds to the psychophysical effect of "pop-out." The effect of the visual context in this case is to decrease the redundancy of many nearly identical stimuli. In contrast, if the visual scene consists of a faded or smudged photograph, the visual system needs to use neighboring visual landmarks to complete incomplete features, such as broken or interrupted lines in the photograph. The effect of visual context here is the enhancement of weak stimuli, rather than the suppression of strong stimuli. Both pop-out and enhancement of weak signals have been studied in the psychophysical literature (4, 5).

We now suggest that both context effects have a neurophysiological correlate at the earliest stage of cortical visual processing, namely in V1. Recalling that the CRF represents a restricted region of visual space, we will denote any visual stimulus within the CRF of a V1 neuron as a center stimulus. Stimuli in the nonclassical receptive field (outside the CRF) will be referred to as surround stimuli.

Modulatory influences of surround stimuli on the response of a cell have been observed in physiological experiments in cats and primates. For high-contrast, well-tuned stimuli inside the CRF, the addition of similar stimuli outside the CRF leads to a suppression of the response (6, 7). On the other hand, when weak (subthreshold) stimuli are present inside the CRF, the addition of multiple similar stimuli in the surround produces a weak increase in the response (6–8).

We propose a model that explains the reversal of the context effect by allowing the net effect of the long-range lateral connections to be stimulus dependent. Specifically, the effect of lateral connections on a center cell is excitatory when the cell receives weak direct input from the lateral geniculate nucleus (LGN), and it is inhibitory when it receives strong input. This effect is a natural consequence of the impact of noisy input on the cell's response and the differential characteristics of excitatory (pyramidal) cells and inhibitory neurons.

The model is a single-layer network of 10,000 excitatory and 10,000 inhibitory cells. Both excitatory and inhibitory cells respond to stimuli of a preferred orientation with individual action potentials. The network map of orientation preferences used was measured by optical imaging in macaque monkey (9) and scaled to the size of the model network. Within each orientation hypercolumn (defined as an aggregate of columns spanning all orientation preferences), excitatory cortico-cortical connections dominate for very nearby cells (10), whereas inhibitory connections are more widely spread (11). Long-range excitatory connections are made onto excitatory and inhibitory cells with similar orientation preferences (Fig. 1) (12).

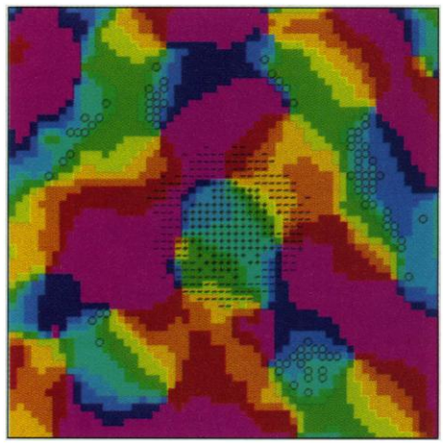

Fig. 1. A 60 by 60 section of the 100 by 100 layer of cells. The preferred orientations of cells are given by a map that was obtained by optical imaging methods in macaque monkey (9). The color of each pixel corresponds to the preferred orientation of the respective cell (yellow, horizontal; green, 45°; red, 90°; and blue, 135°). Power spectral analysis of the scaled orientation map yields a wavelength λ (repeat distance) of 20.6 lattice units. Superimposed in black are the connections made by cells within a circular patch of radius 3 at the center. Predominantly excitatory connections (+); predominantly inhibitory connections (−). Fifty nonorientation-specific local connections are made from each excitatory cell onto excitatory cells within a Gaussian distribution of σ = 2.5 lattice units. Twenty-five connections are made from each inhibitory cell onto excitatory cells within a Gaussian of σ = 1.0 lattice unit. Fifty connections are made from each excitatory cell onto inhibitory cells in a distributed ring ½ lattice units distant. Long-range connections are made from excitatory cells onto both inhibitory and excitatory cells; the centers of these connections are denoted by circles. Each excitatory cell makes 15 long-range connections roughly equally onto excitatory and inhibitory cells between λ and ⅗λ lattice units away. The orientation preferences of target cells are taken from a Gaussian distribution with SD σ = 22.5° centered around the presynaptic cell's preferred orientation.

The LGN input is organized in analogy to stimuli used in physiological studies of nonclassical receptive fields. We idealize the center stimulus as input to cells in one particular orientation column. Stimulation of the nonclassical receptive field (the surround) is simulated by providing input to surrounding hypercolumns. The surround stimulus is oriented either parallel or orthogonal to the center stimulus. The LGN input frequency is taken to be linearly related to stimulus contrast. To test how the modulation by the surround depends on the contrast of the stimulus, we vary the contrast (input rate) of the center stimulus while keeping the contrast of the surround stimuli constant. Figure 2A displays the effect of surround stimuli on the response rate of a typical neuron whose preferred orientation matches the center stimulus.

For high center stimulus contrast, the cell's response is suppressed by about a factor of 2 for orthogonal surround and by nearly a factor of 3 for parallel surround (6). The stronger suppression of cells tuned to the same orientation is a physiological correlate of pop-out: Given the same surround stimulus, the cells that code for the singular (orthogonal) center stimulus respond more strongly.

For low center stimulus contrast, adding a surround stimulus of the same orientation increases the firing rate of the center cells. As shown in Fig. 2B, this increase lowers the perceptual threshold of detecting a stimulus when surrounded by parallel elements (13). The time course of the response is shown in Fig. 2, C and D, comparing a model neuron to the averaged temporal response of real neurons.

Our model accounts for the differing effect of the visual context on the response to weak and strong stimuli using physiologically plausible mechanisms. To analyze the mechanisms responsible for line completion and pop-out, we will consider separately the effect of mean net current and the effect of current fluctuations contributed by the surround.

The net current from the surround contribution depends on the level of activation of the cells responding to the center stimulus (14). Because the spontaneous background input to inhibitory cells in the model is lower than to excitatory cells, inhibitory cells will only be activated at higher external input rates. At low stimulus contrasts, the input from long-range lateral connections will only weakly increase the firing rates of inhibitory neurons; only long-range excitation remains, resulting in the line completion effect. Because the firing rate of inhibitory neurons increases faster than that of excitatory neurons as a function of input, the surround contribution becomes functionally inhibitory as the strength of LGN stimulation increases. The difference between nonorientation- and orientation-specific inhibition is responsible for the pop-out effect.

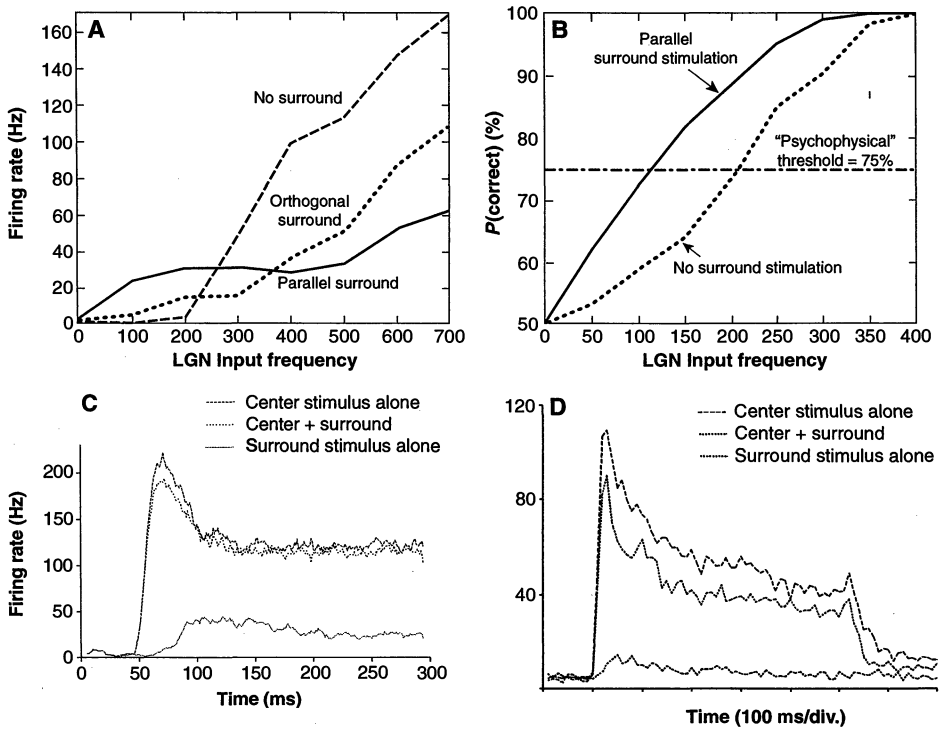

Fig. 2. (**A**) Effect of lateral connections. The average contrast response curves of cells within the classical receptive field are displayed as a function of LGN input frequency (which is assumed to vary linearly with contrast). The central stimulus is always at the preferred orientation. The dashed curve is in the absence of any additional input. The dotted and solid lines were obtained by adding orthogonal and parallel surround stimuli, respectively (see text). Surround input enhances the response frequency for low center input and suppresses it for high center input. The suppression effect is stronger for same-orientation surround input than for orthogonal surround. (**B**) The addition of parallel surround stimulation lowers the detection threshold of the center stimulus at low input contrasts. Three hundred trials were run under each stimulus condition; the variable spike count of one cell within 150 ms of stimulus onset was recorded for each trial. For each surround stimulus condition, the curve represents the probability, given any two trials, one with a center stimulus, and one without, that the trial with the central stimulus produced more spikes than the trial without a central stimulus. (**C**) Post-stimulus time histogram. A smoothed average temporal response of a single unit was computed over 200 trials in response to three stimulus conditions in an artificial (simulated) map on a smaller network: (i) input to preferred orientation within the center hypercolumn (that is, the observed cell) alone (top curve); (ii) simultaneous stimulation of the center at the preferred orientation and the surround at the same orientation (middle curve); and (iii) only surround stimulation (at the preferred orientation of the center); no center stimulation (bottom curve). Stimulus onset occurred at the 50-ms mark. This figure should be compared with the experimental results in figure 15 of Knierim and Van Essen (*6*), reproduced in (**D**) with permission of the *Journal of Neurophysiology*.

Hirsch and Gilbert (*15*) have shown that the analogous experiment of varying the strength of horizontal inputs produces similar results: Threshold microstimulation of the plexus of horizontal fibers results in excitatory postsynaptic potentials (EPSPs), whereas higher stimulus currents evoke disynaptic inhibition that can counter and even overwhelm the laterally evoked EPSP.

As opposed to the common belief that noise is detrimental to information processing, the addition of noise by the surround actually improves the neural sensitivity (at low inputs) by increasing the slope of the response firing rate as a function of the contrast. Using noise to extend the dynamic range of a system is known in physics as stochastic resonance (*16*, *17*).

Even when the net mean current contributed by the lateral connections is always inhibitory (independent of the center stimulus contrast), the fluctuations contributed by the surround can produce an increase in the firing rate for low center contrast (*18*). The differential excitatory and inhibitory cell responses and the response to stochastic input are thus jointly responsible for the context effect.

The context effect mediated by lateral connections described here can serve as a powerful computational mechanism for both line completion and pop-out. In the context of psychophysics, our model predicts that pop-out decreases for weak stimuli. Another model prediction is that the perceived stimulus intensity in the presence of surround stimuli is enhanced for low stimulus contrast and suppressed for high stimulus contrast; this was confirmed psychophysically (*19*). Physiological verification of these predictions requires that stimulus contrast be included as an independent variable in nonclassical receptive field studies (*20*).

REFERENCES AND NOTES

1. V. B. Mountcastle, *J. Neurophysiol.* **20**, 408 (1957); D. Hubel and T. Wiesel, *J. Physiol.* **148**, 574 (1959).
2. C. Gilbert and T. Wiesel, *J. Neurosci.* **3**, 1116 (1983); J. S. Lund, Y. Takashi, J. B. Levitt, *Cereb. Cortex* **3**, 148 (1993); R. Malach, Y. Amir, M. Harel, A. Grinvald, *Proc. Natl. Acad. Sci. U.S.A.* **90**, 10469 (1993).
3. C. Gilbert, *Neuron* **9**, 1 (1992).
4. J. Bergen and B. Julesz, *IEEE Trans. Syst. Man Cybern.* **SMC-13**, 857 (1983).
5. U. Polat and D. Sagi, *Vision Res.* **33**, 993 (1993).
6. J. J. Knierim and D. C. Van Essen, *J. Neurophysiol.* **67**, 961 (1992).
7. A. Grinvald *et al.*, *J. Neurosci.* **14**, 2545 (1994).
8. U. Polat and A. M. Norcia, *Vision Res.*, in preparation.
9. G. Blasdel, *J. Neurosci.* **12**, 3139 (1992).
10. R. Douglas and K. Martin, *J. Physiol.* **440**, 735 (1991); R. Douglas, C. Koch, M. Mahowald, K. Martin, H. Suarez, *Science* **269**, 981 (1995).
11. F. Wörgötter *et al.*, *J. Neurophysiol.* **66**, 444 (1991); D. C. Somers *et al.*, *J. Neurosci.* **15**, 5448 (1995).
12. We chose the same number of inhibitory cells as excitatory cells for reasons of computational efficacy. Each cell's subthreshold membrane potential V obeys the equation $C\,dV/dt = -V/R_{in} + g_E(V^* - V_{Na}) + g_I(V - V_{Cl}) + g_K(V - V_K)$, where C is the membrane capacitance, R_{in} is the cell's input resistance, g_E and g_I are excitatory and inhibitory synaptic conductances, respectively, g_K is a calcium-dependent potassium conductance, and V_{Na}, V_{Cl}, and V_K are the reversal potentials for sodium, chlorine, and potassium, respectively. Spiking is modeled by an integrate-and-fire mechanism in which units that reach a threshold voltage are reset by subtracting the difference between the threshold voltage and the resting potential. The conductance g_E relaxes exponentially and depends on the number of synaptic events impinging on the cell. For unit i, the conductance is $\tau_s\, dg_E/dt = -g_E + \Sigma_j w_{ij}\Theta(V_j - V_{threshold}) + wf_i^0$, where nonzero w_{ij} indicates a connection between units i and j (the synaptic strength is uniform for each synapse type), $\Theta(V_j - V_{threshold})$ is a shorthand notation for whether the unit j spiked in the previous millisecond, and f_i^0 is the external input, which is weighted by w. Local, nonorientation-specific connections serve to implement the massive (excitatory) feedback of the canonical microcircuit (*10*). Inhibitory cells are modeled as receiving fewer projections from LGN and from cortical areas other than pyramidal cells. Without stimulus input, they are further away from firing threshold than the excitatory cells, as indicated by their lower spontaneous firing rate. For each cell type, the external input f_i^0 follows a Poisson distribution and has two components. The first is the stimulus-specific LGN input: Given an input orientation of θ, this component scales as $\cos^2[2(\theta - \theta_i)]$, where θ_i is the cell's preferred orientation. Spontaneous firing results from the second component of f_i^0 that groups together all inputs from outside V1 and LGN. Excitatory cells are subject to firing rate adaptation as given by a simple model of the calcium-dependent potassium conductance: $\tau_K\, dg_K/dt = -g_K + K\Theta(V_i - V_{threshold})$, where K is a positive constant. Spikes arriving from inhibitory cells open conductances with both additive and multiplicative (shunting) effects. The time course of inhibitory conductances is analogous to that for excitatory conductances: $\tau_s\, dg_I/dt = -g_I + \Sigma_j w_{ij}^{inh}\Theta(V_j - V_{threshold}) + w/2f_i^0$. By assuming that inhibition occurs also on the apical shaft of the dendrite, we can model the shunting of excitatory current phenomenologically [following L. F. Abbott, *Physica A* **185**, 343 (1992)] by multiplying the excitatory current by a factor proportional to $\exp(-\sqrt{g_I})$.
13. In analogy to the psychometric curve in two-alternative forced-choice experiments (*5*), we measured in the model network the "neurometric curve" (Fig. 2B) on the basis of spike counts of a single cell within the classical receptive field to verify that the increase in firing results in a lower detection threshold for the central target.

14. The differential response of excitatory and inhibitory cells can be justified physiologically. (i) As a function of the injected current, the firing rate in inhibitory cells increases twice as fast as that in pyramidal cells [D. A. McCormick, B. W. Connors, J. W. Lighthall, D. A. Prince, *J. Neurophysiol.* **54**, 782 (1985)]. (ii) Inhibitory cells in vitro adapt only weakly (*ibid.*). (iii) Successive excitatory post-synaptic potentials (EPSPs) from pyramidal cells onto inhibitory interneurons are potentiated, whereas successive EPSPs from pyramidal cells onto pyramidal cells are depressed [A. M. Thomson and D. C. West, *Neurosci.* **54**, 329 (1993); A. M. Thomson, J. Deuchars, D. C. West, *ibid.*, p. 347]. (iv) Long-range connections terminate in the more distal regions of the dendritic tree of pyramidal cells [L. J. Cauller and B. W. Connors, in *Single Neuron Computation*, T. McKenna, J. Davis, Z. Zornetzer, Eds. (Academic Press, San Diego, 1992), pp. 199–299], and conductances in these regions of high dendritic input resistance are more likely to saturate, or to be shunted [Ö. Bernander, C. Koch, R. J. Douglas, *J. Neurophysiol.* **72**, 2743 (1994)].
15. J. A. Hirsch and C. D. Gilbert, *J. Neurosci.* **11**, 1800 (1991).
16. K. Wiesenfeld and F. Moss, *Nature* **373**, 33 (1995).
17. Signal detection depends on the discrimination between the signal plus noise and noise alone. To first order, the probability of correct classification is proportional to the difference in firing rates $f(I) - f(0)$, where $f(I)$ is the firing rate of the cell in the presence of a center stimulus, and $f(0)$ is the firing rate in its absence. To second order, detection depends on the probability distribution of spike counts over a finite time window. Given a near-threshold center stimulus and a fixed observation time window, the detection probability will peak at an optimal noise level; this peak is termed the "stochastic resonance."
18. For an integrate-and-fire cell, additional input variance results in an increased response to weak subthreshold stimuli, but only a negligible effect on strong stimuli. Integrate-and-fire models capture many of the key features of the discharge curves of real cells in response to noisy current injections [Z. F. Mainen and T. J. Sejnowski, *Science* **268**, 1503 (1995); A. Zador, personal communication]. In these studies, it has been shown that increasing the input variance linearizes the discharge response curve at low firing rates, so that the cell fires even in response to subthreshold input. The fluctuations in the lateral cortico-cortical input current are significant because of the irregularity in the spiking of surround cells. If the surround provides a signal of constant variance and small negative mean, at low stimulus contrast the variance effect will dominate and lower the threshold for detection, whereas at high stimulus contrast the negative mean current will result in the suppression of redundant information in a high-contrast texture background.
19. M. Cannon and S. Fullenkamp, *Vision Res.* **33**, 1685 (1993).
20. D. C. Somers *et al.* have independently developed a model similar to ours [D. Somers, S. Nelson, M. Sur, *Soc. Neurosci. Abstr.* **20**, 1577 (1994)] and verified some of these predictions experimentally [D. C. Somers *et al.*, in *Lateral Interactions in the Cortex*, J. Sirosh and R. Miikkulainen, Eds. (University of Texas, Austin, in press)].
21. Supported by the Howard Hughes Medical Institute, the National Institutes of Mental Health (grants MH47566 and MH45156), the Office of Naval Research, the Air Force Office of Scientific Research, the National Science Foundation, the Center for Neuromorphic Systems Engineering as a part of the National Science Foundation Engineering Research Center Program, and by the Office of Strategic Technology of the California Trade and Commerce Agency. We thank J. Knierim, K. Grieve, F. Wörgötter, and C. Koch for discussions; A. Zador, U. Polat, and M. Sur for access to unpublished data; G. Blasdel for providing the orientation map underlying Fig. 1; and C. Koch and J. McClelland for a stimulating work environment.

3 April 1995; accepted 27 July 1995

An Internal Model for Sensorimotor Integration

Daniel M. Wolpert,* Zoubin Ghahramani, Michael I. Jordan

On the basis of computational studies it has been proposed that the central nervous system internally simulates the dynamic behavior of the motor system in planning, control, and learning; the existence and use of such an internal model is still under debate. A sensorimotor integration task was investigated in which participants estimated the location of one of their hands at the end of movements made in the dark and under externally imposed forces. The temporal propagation of errors in this task was analyzed within the theoretical framework of optimal state estimation. These results provide direct support for the existence of an internal model.

The notion of an internal model, a system that mimics the behavior of a natural process, has emerged as an important theoretical concept in motor control (*1*). There are two varieties of the internal model: (i) forward models, which mimic the causal flow of a process by predicting its next state (for example, position and velocity) given the current state and the motor command; and (ii) inverse models, which invert the causal flow by estimating the motor command that caused a particular state transition. Forward models have been shown to be of potential use for solving four fundamental problems in computational motor control. First, the delays in most sensorimotor loops are large, making feedback control too slow for rapid movements. With the use of a forward model for internal feedback, the outcome of an action can be estimated and used before sensory feedback is available (*2*, *3*). Second, a forward model is a key ingredient in a system that uses motor outflow (also called efference copy) to anticipate and cancel the sensory effects of movement (also called reafference) (*4*). Third, a forward model can be used to transform errors between the desired and actual sensory outcome of a movement into the corresponding errors in the motor command, thereby providing appropriate signals for motor learning (*5*). Similarly, by predicting the sensory outcome of the action without actually performing it, a forward model can be used in mental practice to learn to select between possible actions (*6*). Finally, a forward model can be used for state estimation in which the model's prediction of the next state is combined with a reafferent sensory correction (*7*). Although shown to be of theoretical use, the existence of an internal forward model in the central nervous system (CNS) is still a topic of debate.

When we move an arm in the absence of visual feedback, there are three basic methods the CNS can use to obtain an estimate of the current state—the position and velocity—of the hand. The system can make use of sensory inflow (the information available from proprioception), it can make use of integrated motor outflow (the motor commands sent to the arm), or it can combine these two sources of information by use of a forward model. To test between these possibilities, we carried out an experiment in which participants, after initially viewing one of their arms in the light, made arm movements in the dark. Three experimental conditions were studied, involving the use of null, assistive, and resistive force fields. We assessed the participants' internal estimate of hand location by asking them to localize visually the position of their hand at the end of the movement (*8*). The bias of this location estimate, plotted as a function of movement duration, shows a consistent overestimation of the distance moved (Fig. 1). This bias shows two distinct phases as a function of movement duration: an initial increase reaching a peak of 0.9 cm after 1 s followed by a sharp transition to a region of gradual decline. The variance of the estimate also shows an initial increase during the first second of movement after which it plateaus at about 2 cm^2. External forces had distinct effects on the bias and variance propagation. Whereas the bias was increased by the assistive force and decreased by the resistive force, the variance was unaffected.

These experimental results can be fully accounted for if we assume that the motor control system integrates the efferent outflow and the reafferent sensory inflow. To establish this conclusion, we developed an explicit model of the sensorimotor integration process, which contains as special cases all three of the methods referred to above (*9*). This model is based on the observer framework (*7*) from engineering in which the state estimator (or observer) has access to both the inputs and outputs of the system. Specifically, the input to the arm is the

Department of Brain and Cognitive Sciences, Massachusetts Institute of Technology, Cambridge, MA 02139, USA.

*Present address to which correspondence should be addressed: Sobell Department of Neurophysiology, Institute of Neurology, Queen Square, London WC1N 3BG, UK.